

# Application of Regional Climate Models for Updating Intensity-duration-frequency Curves under Climate Change

**Andre Schardong<sup>1\*</sup> and Slobodan P. Simonovic<sup>2</sup>**

<sup>1</sup>Department of Civil and Environmental Engineering, Western University, 1151 Richmond St, London, ON N6A 3K7, Canada.

<sup>2</sup>Department of Civil and Environmental Engineering and Institute for Catastrophic Loss Reduction, Western University, 1151 Richmond St, London, ON N6A 3K7, Canada.

## **Authors' contributions**

*This work was carried out in collaboration between both authors. Author AS designed the study, performed the statistical analysis and wrote the first draft of the manuscript. Author SPS managed the analyses of the study, assisted with the experiment design, revised the results and the draft manuscript. Both authors read and approved the final manuscript.*

## **Article Information**

DOI: 10.9734/IJECC/2019/V9I530117

### Editor(s):

(1) Dr. Hani Rezgallah Al-Hamed Al-Amoush, Associate Professor, Department of Earth and Environmental, Institute of Earth and Environmental, Al al-Bayt University, Jordan.

### Reviewers:

(1) Davidson Odafe Akpootu, Usmanu Danfodiyo University Sokoto, Nigeria.

(2) Rafael Infante, Caribbean University, Puerto Rico.

Complete Peer review History: <http://www.sdiarticle3.com/review-history/49512>

**Original Research Article**

**Received 23 March 2019**

**Accepted 06 June 2019**

**Published 17 June 2019**

## **ABSTRACT**

Global Climate Models (GCMs) are currently the most powerful tools for accessing changes in the hydrological regime at the watershed scale due to climate change and variability. GCMs, however, have limitations due to their coarse spatial and temporal resolutions. Regional Climate Models (RCMs) are often referred to as suitable alternatives due to their higher resolution of the long-term climate projections. It is expected that RCMs are better for simulating extreme conditions than the GCMs. This present work, investigate the difference in updated IDF (*Intensity-Duration-Frequency*) relationships developed using GCMs and RCMs. The IDF updating method implemented with the *IDF\_CC* tool for Canada has been used for comparison. The analyses are conducted using 369 selected Environment and Climate Change Canada hydro-meteorological stations from the *IDF\_CC* tool database with record length longer than 20 years. Results for the future period (2020-2100), are based on multi-model ensembles of (i) the RCMs from the NA-CORDEX (North-American Coordinated Regional Climate Downscaling Experiment) project

\*Corresponding author: E-mail: [simonovic@uwo.ca](mailto:simonovic@uwo.ca), [aschardo@uwo.ca](mailto:aschardo@uwo.ca);

(ensemble 1) (ii) a sub-set of six GCMs from the GCMs available in the *IDF\_CC* tool used as drivers for the RCMs (ensemble 2) and (iii) all 24 GCMs from the *IDF\_CC* tool database (ensemble 3). One representative concentration pathway (RCP), RCP 8.5, is used in the analysis. The RCMs from the NA-CORDEX project selected for this study use six GCMs as drivers to produce the future predictions for the North American continent, including Canada. Two metrics are applied for the comparison of results: (i) the difference in projected precipitation using the multi-model ensemble median; and (ii) the difference in uncertainty range. The uncertainty range is defined in this study as the percentage projected change in future, 25 to 75 quantiles obtained using the RCMs a GCMs ensembles. The regional models from the NA-CORDEX project generated lower extreme precipitation projections than the GCMs for the stations located in the Canadian prairies (provinces of Alberta, Saskatchewan, Manitoba). Stations located at the East and West coasts of Canada show a smaller difference in the projected extremes obtained using GCMs and RCMs. The use of RCMs shows increase in uncertainty when compared to GCMs. This result indicates that even when using regional climate models, it's advisable to extend the analyses and include as many as possible models from different climate centers.

*Keywords: Regional climate models; IDF curves; CORDEX project; precipitation extremes.*

## 1. INTRODUCTION

The rise in average global surface temperature is attributed to the accelerated human activities and an increase in the concentration of greenhouse gasses in the atmosphere over the last century. Higher atmospheric temperature significantly affects the intensity of extreme rainfall [1-2]. The intensification of the hydrologic cycle caused by the increase in temperature is discussed by many researchers [3-5,7] have presented a comprehensive short-duration extreme precipitation projection mapping for Canada.

Heavy precipitation has been increasing since the 1950s, and it's showing nonuniform spatial distribution [5,7-8]. According to [9], increasing trends in precipitation intensity have been observed over about two-thirds of the northern hemisphere land area. Additionally, a recently published study and noted, with high probability that the average temperature in Canada will increase by the end of the next century and that daily extreme precipitation will likely be more severe [10].

Engineering practice in Canada usually relies on the use of intensity-duration-frequency (IDF) curves for design, maintenance, and operation of water infrastructure. Extreme rainfall change will affect the intensity-duration-frequency (IDF) relationships.

Overcoming the scale mismatch between climate models and watershed observations is one of the significant challenges for the water management professionals. Global Climate Models (GCMs), used for the Coupled Model Intercomparison Project Phase 5 (CMPI5) [11] in the Fifth

Assessment Report (AR5) of the Intergovernmental Panel on Climate Change (IPCC), have resolutions ranging from 1.5° to 3°. Statistical and dynamic downscaling methods [12-15] are applied to cope with this issue and provide for bias correction of the dataset series from the climate models to the observation records at the watershed levels. One of the dynamic downscaling methods is the use of finer-scale Regional Climate Models (RCMs) that produce output series with spatial resolution ranging from 0.11° to 0.5° [16].

In recent years the use and application of regional models have been intensified due to the increasing computational capacity of the climate centers that produce the future predictions using these models. The CORDEX (Coordinated Regional Climate Downscaling Experiment) project coordinates and supports the efforts for the development of regional climate models, including the North American region, NA-CORDEX [17]. NA-CORDEX produces the datasets for the region, including Canada. Many authors have been analyzing and validating the outputs generated by the RCMs including precipitation and temperature projections over the North American continent with a focus on Canada [16,18-20].

In the presented work, a comparative study and analyses are done to investigate the difference in updated IDF relationships developed using GCMs and RCMs from the NA-CORDEX project node. The IDF updating method implemented with the *IDF\_CC* tool [21] for Canada has been used for comparison. Two comparison metrics were used in the study, the difference in projected precipitation using the multi-model

ensemble median and the difference in uncertainty range. The projected changes in the updated IDF relationships are calculated for the selected hydro-meteorological stations series available in the *IDF\_CC* tool's database.

## 2. CLIMATE DATA

### 2.1 Global Climate Models

General Climate Models (GCMs) are developed to represent the dynamics within the Earth's atmosphere to understand current and future climatic conditions. These models are still the best tools for the assessment of climate change impacts. There are a number of GCMs developed by climate research centres around the world. Their simulations are based on (i) land-ocean-atmosphere coupling; (ii) greenhouse gas emissions, and; (iii) different initial conditions representing the state of the climate system. The GCMs usually simulate global climate variables on coarse spatial grid scales ranging from 1.5° to 3° (~150 km to 300 km) and are expected to capture the dynamics of regional-scale climate conditions. The GCMs are designed to predict the climatic variables based on greenhouse gas emissions as the primary variable for generating future conditions. However, other variables such as land-use, energy production, global and regional economy, and population growth are factored-in too to produce the projections.

The AR5 (Fifth Assessment Report) of the IPCC (Intergovernmental Panel on Climate Change) incorporates possible variables affecting the projections and classified the future climate scenarios in distinct Representative Concentration Pathways (RCPs), which are based on time-dependent projections of atmospheric greenhouse gas (GHG) concentrations. The word "representative" signifies that each RCP provides only one of many possible scenarios that would lead to the specific radiative forcing characteristics. The term "pathway" emphasizes that the long-term concentration levels are of interest as well as the expected trajectory to reach the concentration level over time [22].

### 2.2 Regional Climate Models – CORDEX project

The NA-CORDEX dataset provides high-resolution climate change scenario simulation outputs from multiple RCMs (regional climate

models) nested within multiple GCMs (global circulation models) over North America and Canada. The models are run at 0.22° (25 km) and 0.44° (~50 km) spatial resolutions for the period 1950-2005 as the control (historical) period and 2007-2100 as the future period using RCP 4.5 and 8.5. The focus of this study is the RCP 8.5 scenario and RCMs outputs are obtained on the daily time scale. The RCP 4.5 scenario is eliminated due to the significantly smaller number of available datasets. It is also worth mentioning that the CORDEX project produces limited datasets with a grid size of 0.11° [23].

The seven RCMs from the NA-CORDEX project (RCMs CanRCM4, CRCM5-OUR, HIRHAM5, RCA4, RegCM4 and WRF, Mearns et al. [23]) are selected for this study together with six GCMs (CanESM2, EC-EARTH, GFDL-ESM2M, HadGEM2-ES, MPI-ESM-LR and MPI-ESM-MR. [24] as drivers to produce the future predictions. The list of combinations (experiments) is presented in Table 1. The available datasets are provided for two different grid sizes, 0.22° (~25 km) or 0.44° (~50 km). For RCMs without outputs for 0.22° grids, the 0.44° grid resolution is used in the analyses presented in this paper (EC-EARTH GCMs and CanESM2 with RCA4). The combination of GCMs, RCMs and grid sizes, produces a total of 16 datasets for the North American continent for RCP 8.5. The datasets listed in Table 1 were utilized in this work to create the multi-model ensemble for the RCMs and assess the uncertainty ranges.

## 3. METHODOLOGY

Two quantitative comparison metrics are applied to evaluate the results of extreme rainfall statistics for Canada from two distinct climate products used for updating IDF curves under climate change. The first is a subset of global climate models available with the *IDF\_CC* tool that corresponds to the drivers for the NA-CORDEX project runs, and the second is the dataset of the regional climate models (RCMs) itself. Precipitation downscaling method of the *IDF\_CC* tool [6,21,25-26] is used for updating the IDF relationships for climate change. The *IDF\_CC* tool methodology is briefly presented in the following section. Details on the methodology implemented with the *IDF\_CC* tool are given in [21], the *IDF\_CC tool Technical Manual* [25], and the *IDF\_CC tool Users' Manual* [27].

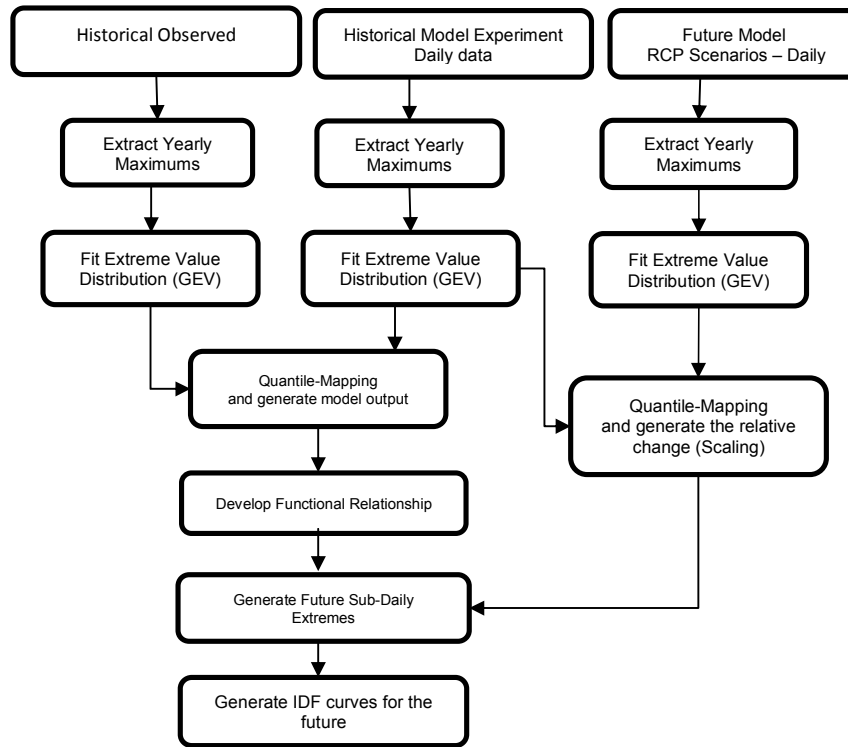


Fig. 1. Flowchart of the Equidistance Quantile-Matching (EQM) method for generating future IDF curves under climate change in the IDF\_CC tool version 3.5 (adopted from [25])

Table 1. Regional climate models - NA-CORDEX dataset

	Driver – GCM	Model - RCM	Grid size
1	CanESM2	CanRCM4	0.22°
2		CRCM5-OUR	0.22°
3		CRCM5-UQAM	0.22°
4		RCA4	0.44°
5	EC-EARTH	HIRHAM5	0.44°
6		RCA4	0.44°
7	GFDL-ESM2M	CRCM5-OUR	0.22°
8		RegCM4	0.22°
9		WRF	0.22°
10	HadGEM2-ES	RegCM4	0.22°
11		WRF	0.22°
12	MPI-ESM-LR	CRCM5-OUR	0.22°
13		CRCM5-UQAM	0.22°
14		RegCM4	0.22°
15		WRF	0.22°
16	MPI-ESM-MR	CRCM5-UQAM	0.22°

**3.1 IDF\_CC Tool Description – Precipitation Downscaling**

The *IDF\_CC* public domain tool is developed by the University of Western Ontario and maintained by the Institute for Catastrophic Loss Reduction with currently over 2,100 registered and active users in Canada ([www.idf-cc-uwo.ca](http://www.idf-cc-uwo.ca)). It is

developed as a generalized decision support system (DSS) able of generating IDF curves by incorporating the effect of climate change. It provides precipitation intensities and accumulation depths for the following durations: 5, 10, 15, 20, 30 minutes, 1, 2, 6, 12 and 24 hours, and return periods: 2, 5, 10, 25, 50 and 100-year. The tool enables users to generate IDF

curve information based on observation records and the future climate projections using precipitation series from the GCMs [6, 21, 28].

The *IDF\_CC* tool version 3.5 adopts a modified version of the equidistant quantile-matching (EQM) method of [13] for temporal downscaling of precipitation data which can capture the distribution of changes between the projected period and the baseline. Future projections are incorporated by using the concept of quantile delta mapping [29-31], also known as scaling. For spatial downscaling, version 3.5 of the tool utilizes data from GCMs produced for Coupled Model Inter-comparison Project Phase 5 - CMIP5 [32].

### 3.1.1 IDF curves under changing climate

A very common assumption in developing IDF curves is the stationarity of the precipitation time series. Under the changing climate, this assumption may result in misrepresentation of future extreme conditions, and therefore, the development of IDFs for future climate should not rely only on historical observations [33-34]. Global Climate Models (GCMs) are one of the best ways to explicitly address changing climate conditions for future periods (i.e., non-stationarity condition). GCMs simulate atmospheric patterns on larger spatial grid scales (usually greater than 100 kilometres) and are therefore unable to represent the regional scale dynamics accurately. In contrast, the regional climate models (RCMs) are developed to incorporate the local-scale effects and use smaller grid scales, usually 10 to 50 kilometres or even less. The main shortcoming in the use of RCMs is the computational intensity required to generate realizations for various atmospheric forcing.

Both GCMs and RCMs usually present spatial scales larger than the size of most urban and rural watersheds in which the IDF curves are used for the design of critical urban drainage infrastructure, drainage systems for roads, etc [35-37]. The downscaling techniques link GCM/RCM grid scales and local study areas for the development of IDF curves under changing climate conditions. Downscaling approaches are commonly classified as either dynamic or statistical. The dynamic downscaling procedures are based on higher resolution climate models (RCMs) to simulate extreme events with higher accuracy. Statistical downscaling methods are based on transfer functions or mapping schemes, which relate GCM outputs with the locally observed data. Statistical downscaling

has lower computational burden than dynamic and therefore is usually the preferred approach in engineering practice. Additionally, the GCM outputs are available for a broader range of emission scenarios than the RCM outputs.

### 3.1.2 Equidistant quantile matching method with GEV

The *IDF\_CC* tool uses an equidistant quantile matching (EQM) downscaling method to update the IDF curves under changing climate conditions by temporally downscaling precipitation data to incorporate the changes of the GCM projections, between the baseline period (or control/historical run) and the future period. The flow chart of the EQM methodology is shown in Fig. 1. The statistical distribution used is the General Extreme Value Distribution (GEV) that combines three other continuous distributions into one: Gumbel (EV1), Fréchet (EV2) and Weibull (EV3). The GEV has three parameters, namely location, scale and shape. The shape parameter governs the type of distribution (EV1, EV2 or EV3 [38-41]). With the three parameters, the GEV distribution fits better the extreme precipitation series than the Gumbel distribution with two parameters used by ECCC [40,42-44].

### 3.2 Climate Data Ensembles

Results are produced and presented for three datasets (multi-model ensembles), that are defined as follows: *Ensemble 1*: for the RCMs dataset as in Table 1, *Ensemble 2* for the ensemble of the six selected GCMs used as drivers for the RCMS (Table 1) and *Ensemble 3* for the dataset of all 24 GCMs (see Appendix 1 for the complete list) available in the *IDF\_CC* tool database. Results are produced for the RCP scenario 8.5.

### 3.3 Comparison Metrics

For the comparison of the updated IDF relationships using three described ensembles datasets, two metrics are applied to compute (i) the difference between projected changes in total precipitation, and (ii) the uncertainty range (defined as the difference between IDF relationships obtained using different climate datasets).

The difference in total projected precipitation metric (Metric 1:  $\Delta\text{Change } \%$ ), is calculated as:

$$\text{Metric 1: } \Delta\text{Change } (\%) = CP_{RCM} - CP_{GCM,i} \quad (1)$$

where  $CP_{RCM}$  the change on precipitation projected by the ensemble median of the RCMs and  $CP_{CGM,i}$  is the change in precipitation projected by the multi-model ensemble median of the GCMs and the subscript  $i$  represents the ensemble (2 or 3) used.

The difference in projected uncertainty (Metric 2:  $\Delta U_{nc}$  %), is calculated by the following metric:

$$\text{Metric 2: } \Delta U_{nc} (\%) = (CQ_{75,RCM} - CQ_{25,RCM}) - (CQ_{75,CGM,i} - CQ_{25,CGM,i}) \quad (2)$$

where  $CQ_{q25,RCM}$  and  $CQ_{q75,RCM}$  are the 25<sup>th</sup> and 75<sup>th</sup> quantiles, respectively, of the range of changes in precipitation projected using the RCMs and  $CQ_{q25,CGM}$  and  $CQ_{q75,CGM}$  are the 25th and 75th quantiles, respectively, of the changes in precipitation projected using the GCMs, and the subscript  $i$  represents the ensemble (2 or 3) used.

**Error! Reference source not found.** presents a flowchart of the procedure used for the calculation of the comparison metrics using the three distinct climate datasets.

### 3.4 Experiments Setup

For the analyses presented in this paper, IDF curves were calculated for 369 selected stations from [45], version 3.0 of the dataset, with the length of observed data of at least 20 years, and available with the *IDF\_CC* tool database. Fig. 3 presents the locations of ECCC stations used in this study, highlighting the distribution of stations across the country. The blue dots in Fig. 3 represent the selected precipitation gauging stations for the analyses. The presented map clearly shows an uneven distribution of stations across Canada. The higher density of data records is available at the east coast of Canada, in the southern regions of the provinces of Ontario and Quebec, followed by the province of British Columbia, on the west coast. The northern regions of the BC (British Columbia), ON (Ontario) and QC (Quebec) and the other provinces and territories of the country have lower density of stations. The analyses presented in this study are conducted for the EC stations, and therefore, the results presented are less representative for the regions with sparse stations coverage.

For the comparison purposes, 2 and 24 hours duration and 25- and 100-year return period IDF curves are used. They are often used in Canadian municipal engineering practice for stormwater drainage and flood risk management. The *IDF\_CC* tool provides for very efficient IDF calculations for multiple return periods (2, 5, 10, 25, 50 and 100-year) and durations (5, 10, 15 and 30 minutes and 1, 2, 6, 12 and 24 hours).

Table 2 presents a summary of all analyses performed in this study. The experiments listed in Table 2 are conducted using both climate products (GCMs and RCMs). The complete analyses of all outputs are created as PDF files and are available as supplemental material.

The complete set of maps for all stations included in the analyses were created for the return periods (RT) and durations mentioned above. The comparison metrics presented in the discussion include only 25- and 100-year return periods, and 2 and 24 hours durations. All other maps, histograms and summaries, are available as supplemental material.

The IDF values are calculated for each station using the historical data and future climate conditions for the three listed ensembles. Two types of maps are generated and discussed: (a) projected changes in future extreme precipitation for RCMs and GCMs and the difference between the projections including a linear regression and diagnostic plots (residuals vs. fitted values, Q-Q, scale location and Cook's distance plots); and (b) difference between projected uncertainty range for RCMs and GCMs.

## 4. RESULTS AND DISCUSSION

The precipitation projected for the IDF curves using the RCMs (ensemble 1) and the GCMs (ensembles 2 and 3), and the differences in total precipitation change (metric 1) and the uncertainty (metric 2) are presented and discussed in this section. The circles shown in the Fig. 4 represent the differences calculated using metric 1 and 2.

The circles shown in the maps represent the geographical location of the stations and the value associated with each site is influencing the size (the larger the absolute value, the larger the size of the circle). Each map has its own scale.

**Table 2. Summary of the analyses performed in the study**

Climate Data	Design criteria		Ensemble		
	2 hours 25-year	24 hours 100-year	1. RCMs	2. Six selected GCMs	3. All 24 GCMs
Historical	X				
Future projections	X	X	X		
	X			X	
	X				X
		X	X		
		X		X	
		X			X

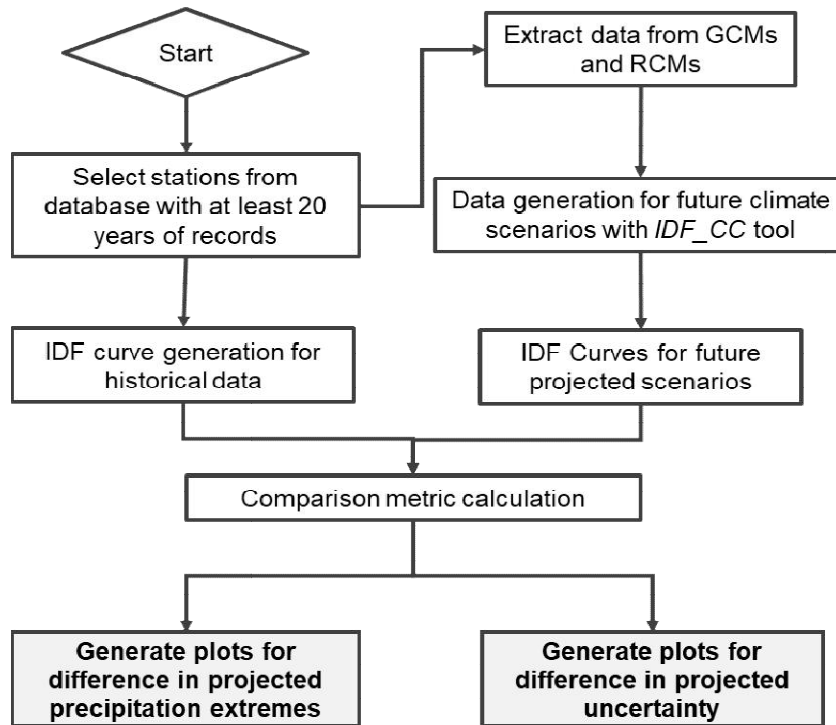


**Fig. 2. Flowchart of the applied comparison methodology**

The colour scale ranges from a dark blue for negative values to a dark red for highest positive values, whereas light blue and light red/yellow colours indicate values closer to the median of the corresponding scale on the map.

**4.1 Projected Precipitation Analyses**

In this section, the analyses are carried out using the median values from the three ensembles for the experiments listed in Table 2. Therefore, the reference to the ensemble number always concerns median value obtained from the set of models included in the ensemble.

The correlation between the results from the three different ensembles was tested by fitting a linear model to changes projected for each station. The regression model is fitted for the difference between historical and projected precipitation for ensembles 1 and 2 (Fig. 6a), and for ensembles 1 and 3 (Fig. 6b) for 24 hours (1440 min) duration, 100-year return period and RCP 8.5 using the multi-model ensemble (median value), for projected period 2020-2100. The results show a high pairwise correlation between the projections of RCMs and GCMs and only a few instances (stations) with higher leverage, according to Fig. 6. However, with a

Cook's distance much lower than 0.5, indicating the absence of apparent outliers.

**4.1.1 Difference in projected precipitation between RCMs and GCMs**

The results in Fig. 7, show the difference between extreme projected precipitation calculated using metric 1 (eq. 1) for RCP 8.5, 2 hours (120 min) duration, 25-year return period, for ensembles 1 and 2 (Fig. 7a) and ensembles 1 and 3 (Fig. 7b). In the first case, the difference in projections ranges from -19.30% to +15.28% with the mean of -2.17 %, indicating that the ensemble 1 is projecting a slightly lower increase in future extreme precipitation than ensemble 2. In the second experiment, using ensembles 1 and 3 (Fig. 7b), the differences range from -12.12% up to +16.08% with the mean of -0.52%, indicating, that on average there is no significant difference between projections from RCMs (ensemble 1) and GCMs ensembles (2 and 3).

However, there is a spatial variation in the projected difference between the GCMs and RCMs as can be observed in Fig. 7a. The RCMs are projecting lower increase in precipitation than the GCMs, especially over the east coast of Canada. In the northern regions of the province

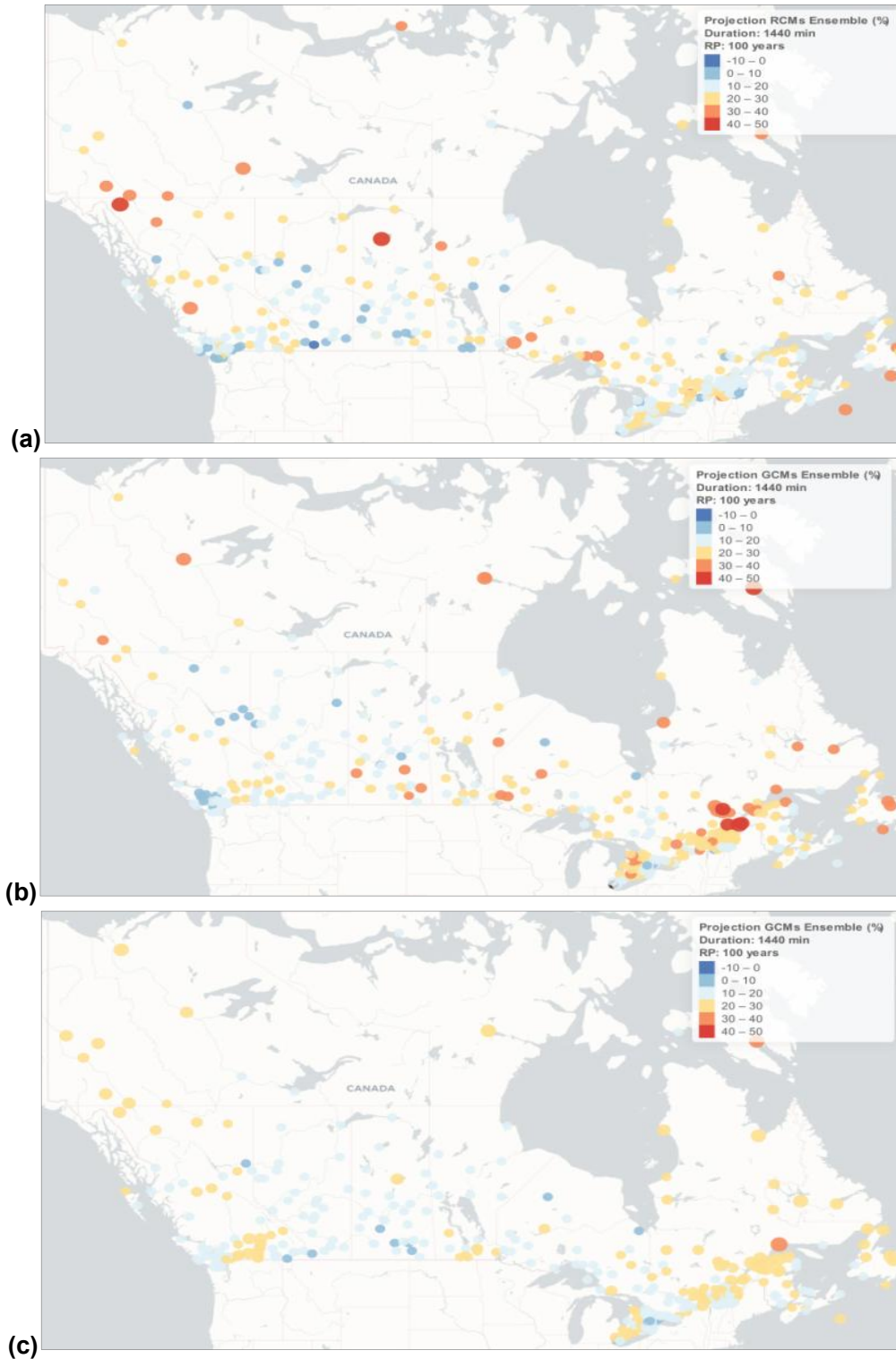
of Ontario and prairies, the RCMs tend to produce slightly higher projections than the GCMs and a neutral trend on the west coast of the country. The results for the analysis using ensembles 1 and 3 is presented in Fig. 7b, and the spatial pattern is very similar to the previous experiment. This is expected, since these two maps are made using the median values as representative of the ensembles.

Fig. 8 presents the same experiment set up as in Fig. 7 for 24 hours (1440 min) duration and 100-year return period projected precipitation. The difference in projections between ensembles 1 and 2 (Fig. 8a) ranges from -30.86% up to +28.00% with the mean of -2.53%, and the difference between ensembles 1 and 3, ranges from -20.23% up to +28.00% with the mean of -0.34%. Similar spatial behaviour is observed, with mixed trend on the west coast of Canada.

The histogram of both experiments, differences between the projected precipitation for the future period between ensembles 1 and 2 (Fig. 9a) and ensembles 1 and 3 (Fig. 9b) for 2 hours duration and 25-year return period, and ensembles 1 and 2 (Fig. 9c) and ensembles 1 and 3 (Fig. 9d) for 24 hours duration and 100 years return period.



**Fig. 3. Locations of the selected ECCC stations used in the analyses**

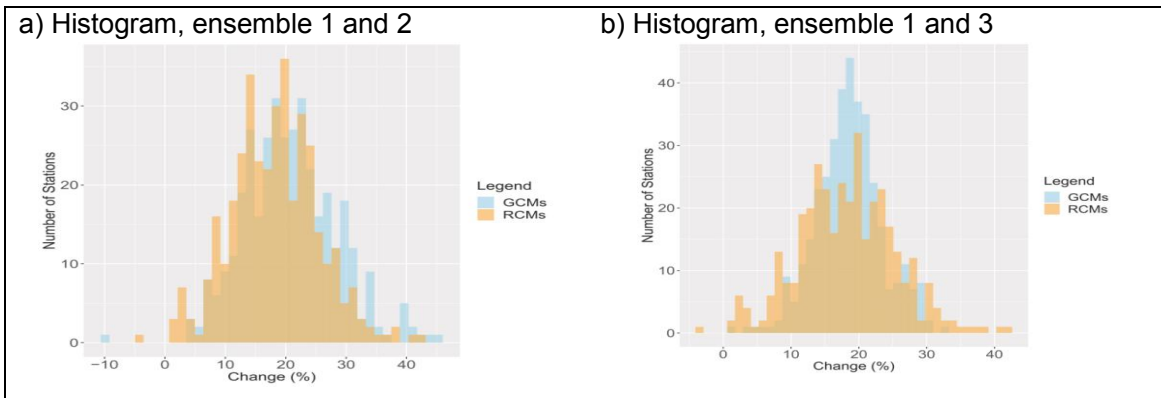


**Fig. 4. Difference between historical and projected precipitation for the ensemble 1 (a), ensemble 2 (b) and ensemble 3 (c) for 24 hours (1440 min) duration, 100-year return period and RCP 8.5. The values are generated using the *IDF\_CC tool* with multi-model ensemble (median value) and projected period 2020-2100**

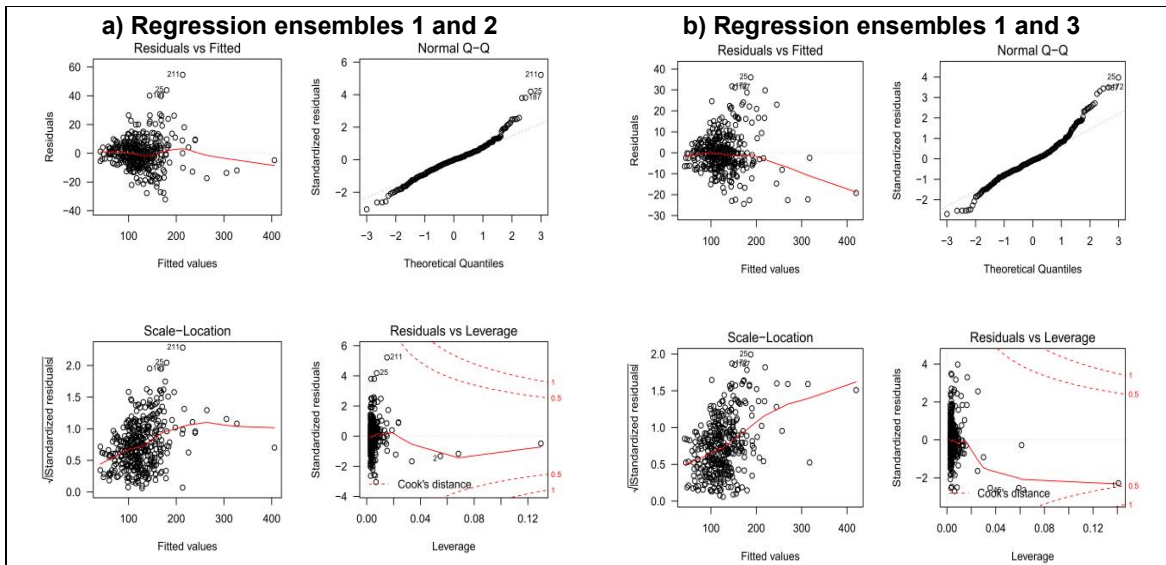
### 4.1.2 Uncertainty range analyses

The difference in the uncertainty range of the projected change in the precipitation extremes between the ensembles 1 and 2, is presented in Fig. 10a. The plot shows the results for 2 hours duration and 25-year return period and RCP8.5. The difference in percent uncertainty calculated using metric 2 (eq. 2) ranges from -15.88% to +25.99%, with the mean of +5.05% considering all stations across Canada. For the experiment comparing the differences between ensembles 1

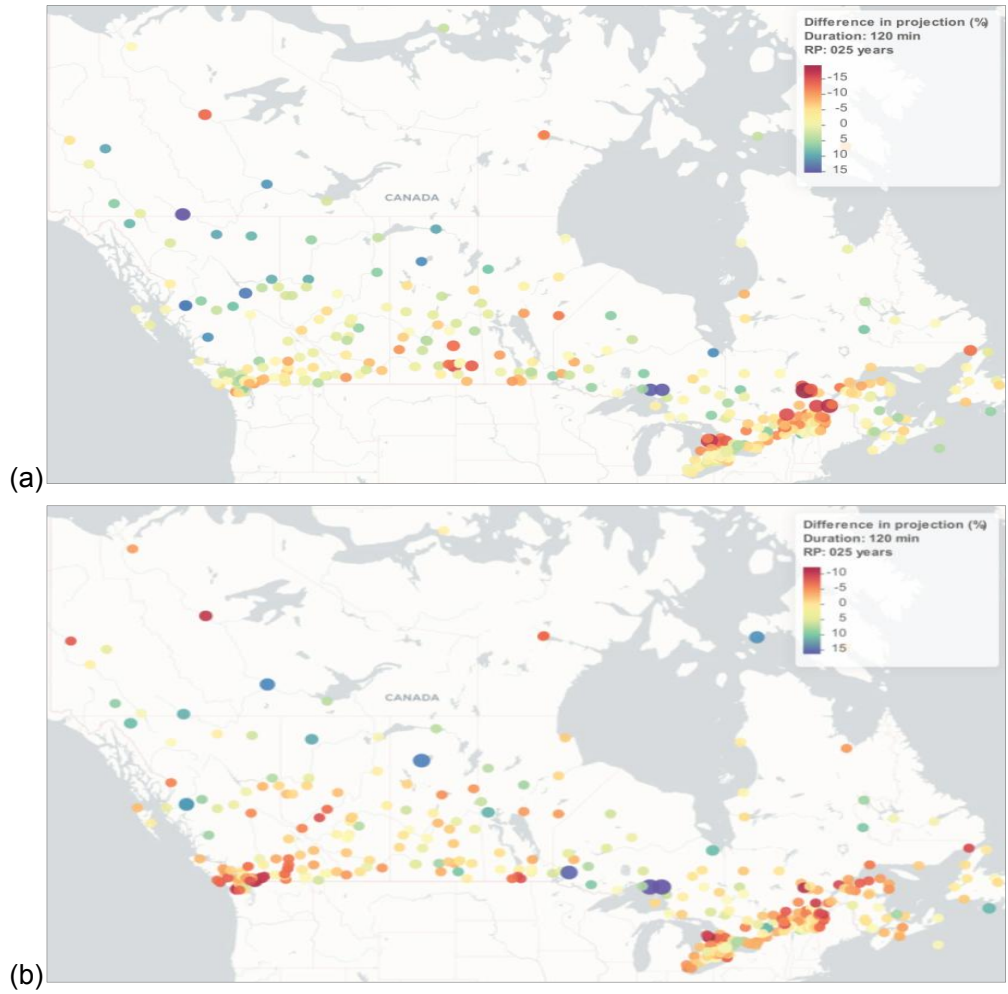
and 3 (Fig. 10b) the difference in uncertainty ranges from -10.96% to +24.94% with the mean of +3.84%. Negative values indicate that the RCMs produce lower uncertainty than the GCMs. The experiments presented in Fig. 10 are repeated for 24 hours duration and 100-year return period and the results are shown in Fig. 11. The difference in uncertainty range for ensemble 1 and 2 from -36.06% to +34.15% with the mean of +6.95% and for the experiment comparing ensembles 1 and 3 ranges are from -19.87% up to +34.39% with the mean of +5.82%.



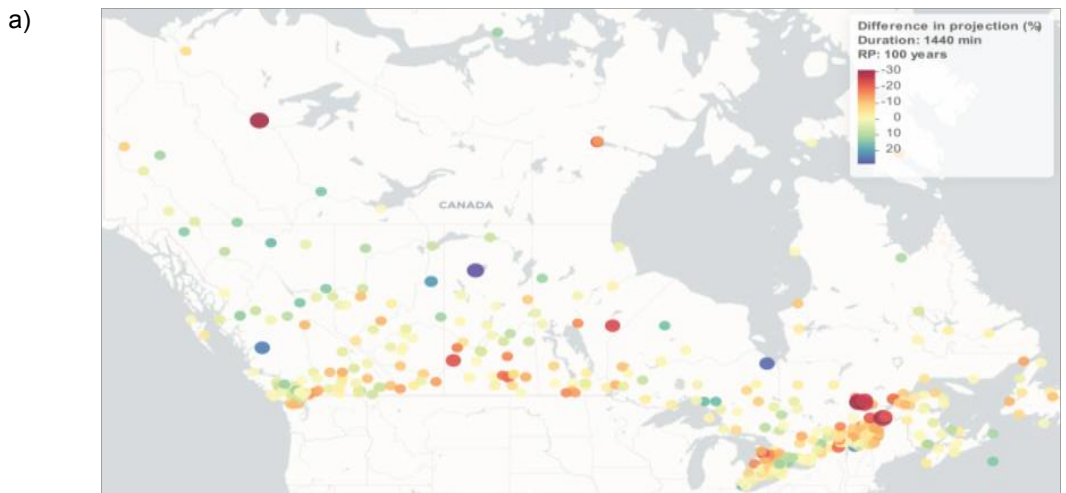
**Fig. 5. Histograms of the difference between historical and projected precipitation for ensemble 1 and 2 (a), and ensemble 1 and 3 (b) for 24 hours (1440 min) duration, 100-year return period and RCP 8.5 using the multi-model ensemble (median value)**

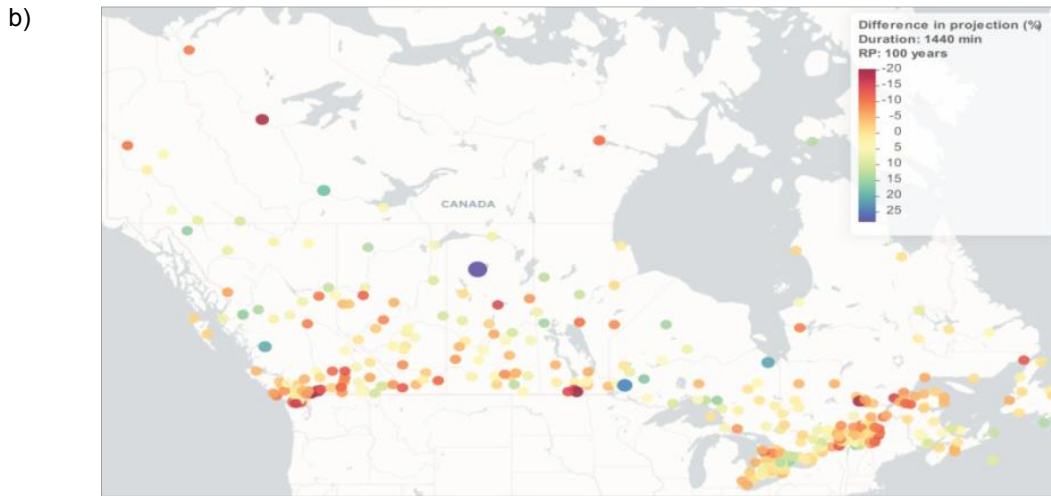


**Fig. 6. Linear regression and diagnostic plots for the percent difference between ensembles 1 and 2 (a) and ensembles 1 and 3 (b) in projected precipitation changes for 24 hours (1440 min) duration, 100-year return period and RCP 8.5 using the multi-model ensemble (median value), for projected period 2020-2100**

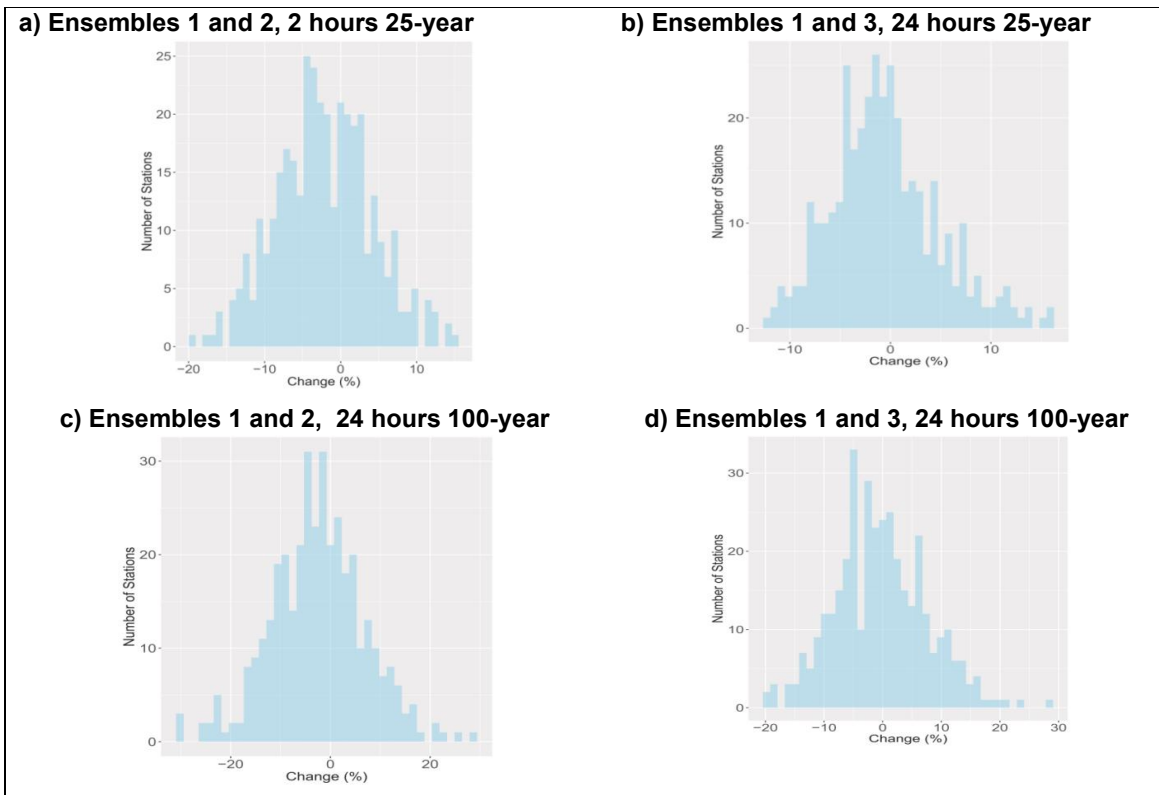


**Fig. 7. Percent difference between ensembles 1 and 2 (a) and ensembles 1 and 3 (b) in projected precipitation changes for 2 hours (120 min) duration, 25-year return period and RCP 8.5 using the multi-model ensemble (median value), using metric 1 and projected period 2020-2100**

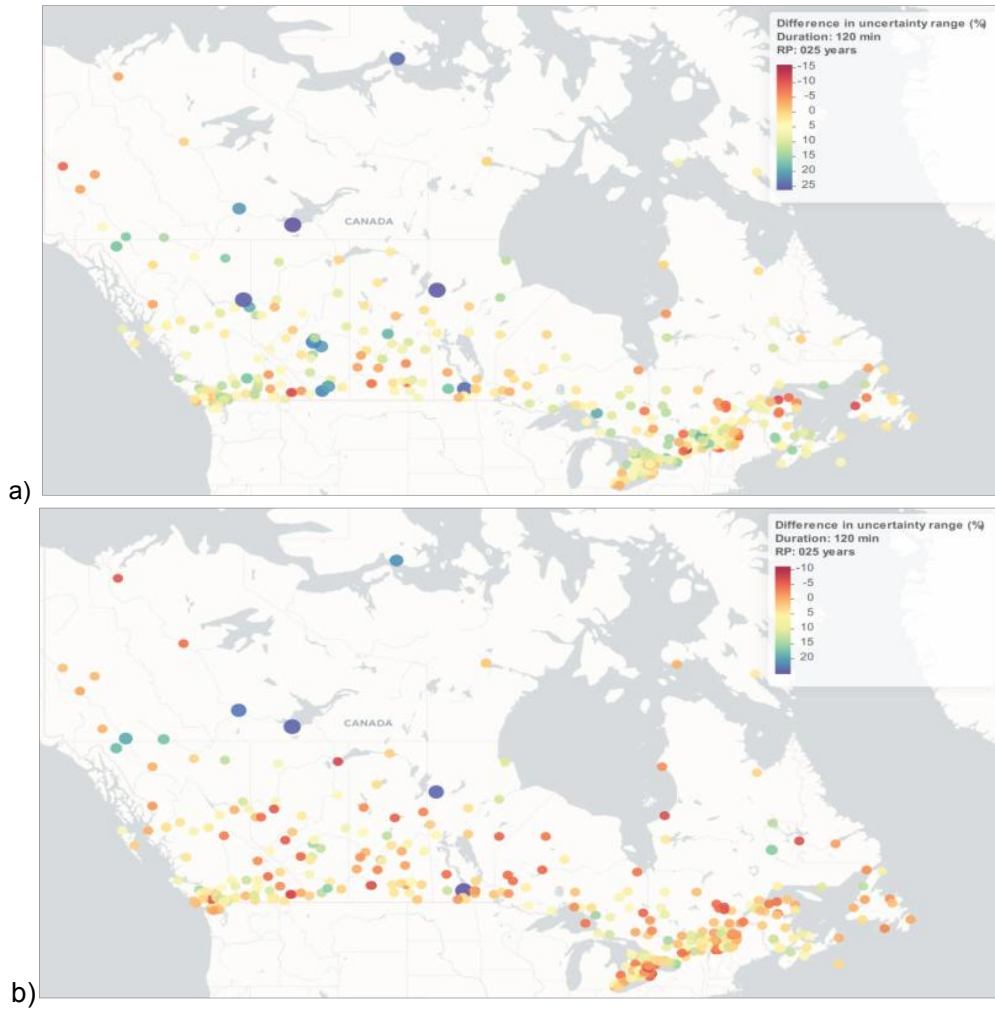




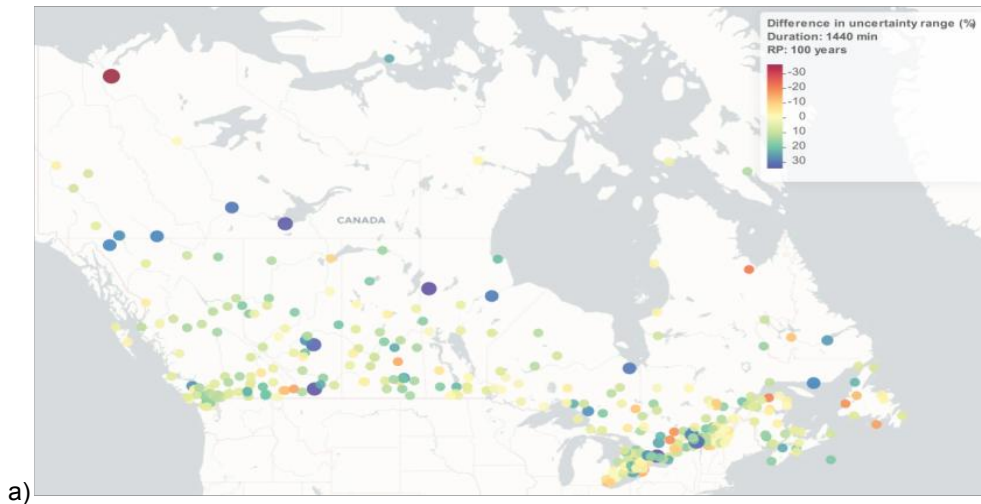
**Fig. 8. Percent difference between ensembles 1 and 2 (a) and ensembles 1 and 3 (b) in projected precipitation changes for 24 hours (1440 min) duration, 100-year return period and RCP 8.5 using the multi-model ensemble (median value), using metric 1 and projected period 2020-2100**



**Fig. 9. Histograms of the difference between the projected precipitation for the future period from the ensembles 1 and 2 (a) ensembles 1 and 3 (b) for 2 hours duration and 25-year return period, and ensembles 1 and 2 (c) and ensembles 1 and 3 (d) for 24 hours duration and 100 years return period**



**Fig. 10. Percent difference in the projected uncertainty between ensembles 1 and 2 (a) and ensembles 1 and 3 (b) for 2 hours (120 min) duration, 25-year return period and RCP 8.5, and projected period 2020-2100 using the multi-model ensemble median values, for metric 2.**



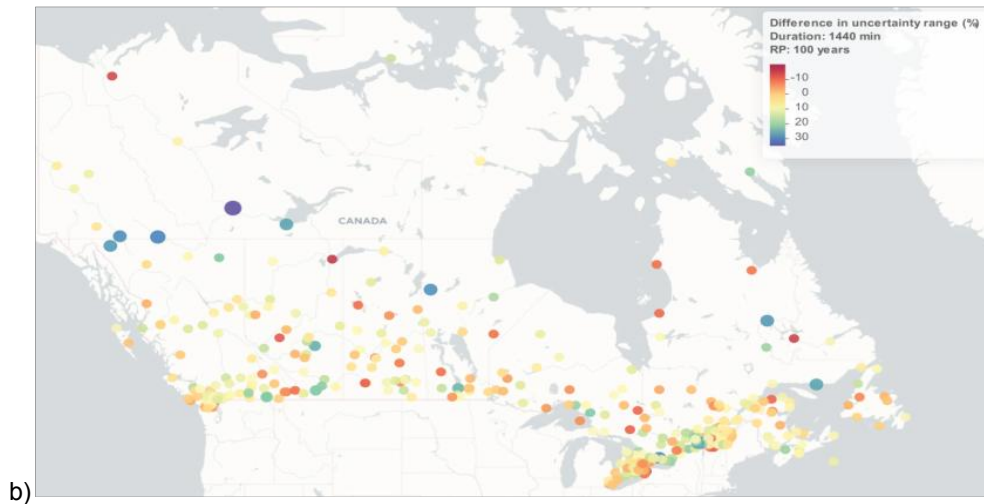


**Fig. 11.** Percent difference in the projected uncertainty between ensembles 1 and 2 (a) and ensembles 1 and 3 (b) for 24 hours (1440 min) duration, 100-year return period and RCP 8.5, and projected period 2020-2100 using the multi-model ensemble (median value), for metric 2

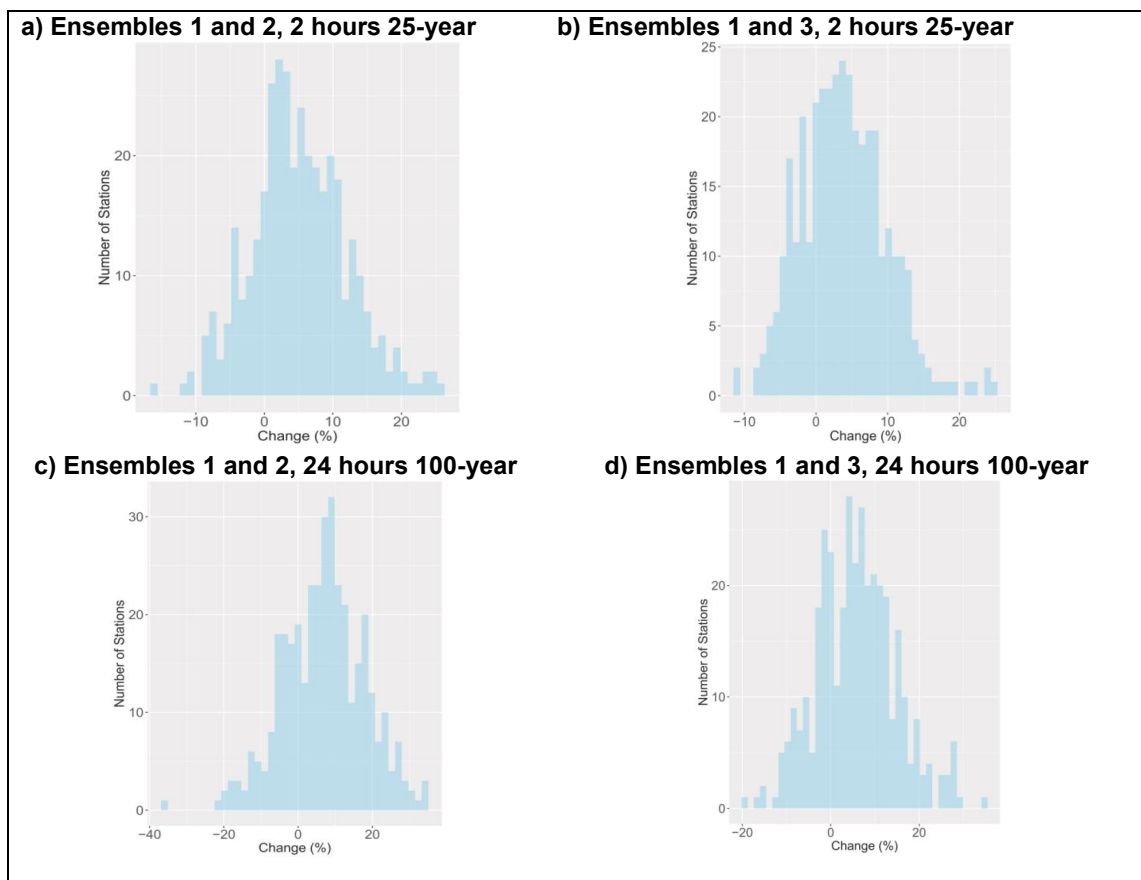


**Fig. 12.** Histograms for the differences in the projected IDF range of uncertainty for 2 hours duration, 25-year return period and RCP 8.5 for metric 2 between ensembles 1 and 2 (a) and ensembles 1 and 3 (b) using the multi-model ensemble, and for 24 hours duration and 100-year return period for ensembles 1 and 2 (c) and ensembles 1 and 3 (d)

Fig. 12 presents the histogram for the differences in uncertainty for all stations across Canada for the four experiments conducted: Fig. 12a and b, show the histograms for the 2 hours duration and 25-year return period for the experiments comparing ensembles 1 and 2, and ensembles 1 and 3, respectively and Fig. 12c and d the 24 hours duration and 100-year return period experiments, also for ensembles 1 and 2 and ensembles 1 and 3, respectively. The histograms presented match the results shown on the maps, indicating that GCMs ensemble result in lower uncertainty than the RCMs. This is a clear indication that using the outputs from regional climate models may not assist in reducing the uncertainty in future climate projections.

## 5. CONCLUSIONS

This manuscript presents an analysis of the results obtained from the application of the *IDF\_CC* tool developed by Simonovic et al. (2016) with three climate datasets, one using the RCMs from the NA-CORDEX project (ensemble 1), a second using a sub-set of six GCMs from the GCMs available in the *IDF\_CC* tool used as drivers for the RCMs (ensemble 2) and a third with all 24 GCMs from the *IDF\_CC* tool database (ensemble 3). The emission scenario explored in the analyses is RCP8.5. The analyses have been performed for durations: 5, 10, 20, 15, 30 minutes, 1, 2, 6, 12, 24 hours, and return periods 2, 5, 10, 25, 50 and 100-year, and all 24 GCMs available in the *IDF\_CC* tool database. Due to the large volume of obtained results, two representative storm events were discussed in this paper: a short duration high-frequency event (2 hours 25-year event) frequently used for urban stormwater management applications, and a long duration low-frequency event (24 hours, 100-year event) used in the management of flood risk in Canada.

The *IDF\_CC* tool includes more than 700 ECCC hydrometeorological stations to assist local water managers in the development of climate change affected IDFs. In this study, however, 369 of them were selected for the analyses with a minimum record length of 20 years.

The results presented show a strong correlation between the projected changes in IDF curves using the RCMs and GCMs, for both of the experiment (ensemble 1 and ensemble 2 and ensemble 1 and 3). Additionally, on average, the use of RCMs results in lower increase in extreme precipitation, consequently smaller increase in

the IDF curves. In previous studies (Simonovic et al., 2016 and 2017) there was a concern that the interpolation of data from the coarser GCM grids may be causing a smoothing of the extreme values of projected precipitation. With this study, we confirm that the bias correction introduced by the quantile matching method used in the *IDF\_CC* tool is overcoming this shortcoming, given the fact that this projection from the GCMs are more conservative than the RCMs.

The analyses of the uncertainty show that the use of RCMs included in the current study, presented, in general, a larger uncertainty value than the GCMs in both cases (ensembles 2 and 3). Therefore, only using a single RCM for a climate change adaptation studies is not recommended, even when it is believed that regional models can reduce the uncertainty in future projections obtained from the use of global climate models.

## COMPETING INTERESTS

Authors have declared that no competing interests exist.

## REFERENCES

1. Westra S, Alexander L, Zwiers F. Global increasing trends in annual maximum daily precipitation. *Journal of Climate*. 2013; 26(11):3904-3918. DOI: 10.1175/jcli-d-12-00502.1
2. Westra S, Fowler H, Evans J, Alexander L, Berg P, Johnson F, et al. Future changes to the intensity and frequency of short-duration extreme rainfall. *Reviews of Geophysics*. 2014;52(3):522-555. DOI: 10.1002/2014rg000464
3. Huntington T. Evidence for intensification of the global water cycle: Review and synthesis. *Journal of Hydrology*, 2006; 319(1-4):83-95. DOI: 10.1016/j.jhydrol.2005.07.003.
4. Held I, Soden B. Robust responses of the hydrological cycle to global warming. *Journal of Climate*. 2006;19(21):5686-5699. DOI: 10.1175/jcli3990.1
5. Warren FJ, Lemmen DS. Canada in a changing climate: Sector perspectives on impacts and adaptation. Government of Canada, Ottawa, ON. 2014;286.
6. Simonovic SP, Schardong A, Sandink D. Mapping extreme rainfall statistics for Canada under climate change using

- updated intensity-duration-frequency curves. *ASCE Journal of Water Resources Planning and Management*. 2017;143(3): 1943-5452.  
DOI: 10.1061/(ASCE)WR.0000725
7. Kharin VV, Zwiers FW, Zhang X, Wehner M. Changes in temperature and precipitation extremes in the CMIP5 ensemble. *Clim. Change*. 2012;119(2):345–357.
  8. Min S, Zhang X, Zwiers FW, Hegerl GC. Human contribution to more-intense precipitation extremes. *Nature*. 2011;470: 378–381.  
DOI: 10.1038/nature09763
  9. Zwiers FW, Zhang X, Feng Y. Anthropogenic influence on long return period daily temperature extremes at regional scales. *J. Clim*. 2011;24:881-892.
  10. Zhang X, Flato G, Kirchmeier-Young M, Vincent L, Wan H, Wang X, Rong R, Fyfe J, Li G, Kharin VV. Changes in temperature and precipitation across Canada; Chapter 4 in Bush E, Lemmen DS. (Eds.) *Canada's Changing Climate Report*. Government of Canada, Ottawa, Ontario. 2019;112-193.
  11. Taylor KE, Stouffer RJ, Meehl GA. An overview of CMIP5 and the experiment design. *Bull Am Met Soc*. 2012;93(4):485–498.
  12. Hassanzadeh E, Nazemi A, Elshorbagy A. Quantile-based downscaling of precipitation using genetic programming: Application to IDF curves in Saskatoon. *J Hydrol Eng*. 2013;19:943–955.  
DOI: 10.1061/(ASCE)HE.1943-5584.0000854
  13. Srivastav RK, Schardong A, Simonovic SP. Equidistance quantile matching method for updating IDF curves under climate change. *Water Resour Manage*. 2014;28(9):2539-2562.  
DOI: 10.1007/s11269-014-0626-y
  14. Cannon AJ, Sobie SR, Murdock TQ. Bias correction of GCM precipitation by quantile mapping: How well do methods preserve changes in quantiles and extremes? *J. Climate*. 2015;28:6938–6959.  
Available:https://doi.org/10.1175/JCLI-D-14-00754.1
  15. DeGaetano AT, Castella no CM. Future projections of extreme precipitation intensity-duration-frequency curves for climate adaptation planning in New York State. *Clim Serv*. 2017;5:23–35.  
DOI: 10.1016/j.cliser.2017.03.003
  16. Diaconescu EP, Mailhot A, Brown R, et al. Evaluation of CORDEX-arctic daily precipitation and temperature-based climate indices over Canadian Arctic land areas. *Clim Dyn*. 2018;50:2061.  
Available:https://doi.org/10.1007/s00382-017-3736-4
  17. Mearns et al; 2017.
  18. Whan K, Zwiers F. Evaluation of extreme rainfall and temperature over North America in CanRCM4 and CRCM5. *Clim Dyn*. 2016;46:3821.  
Available:https://doi.org/10.1007/s00382-015-2807-7
  19. Lucas-Picher P, Laprise R, Winger K. Evidence of added value in North American regional climate model hindcast simulations using ever-increasing horizontal resolutions *Clim Dyn*. 2017;48: 2611.  
Available:https://doi.org/10.1007/s00382-016-3227-z
  20. Jeong II, Sushama LD. Rain-on-snow events over North America based on two Canadian regional climate models. *Clim Dyn*. 2018;50:303.  
Available:https://doi.org/10.1007/s00382-017-3609-x.
  21. Simonovic SP, Schardong A, Sandink D, Srivastav R. A web-based tool for the development of intensity duration frequency curves under changing climate. *Environmental Modelling & Software Journal*. 2016;81:136-153.
  22. Moss RH, Edmonds JA, Hibbard KA, Manning MR, Rose SK, van Vuuren DP, Carter TR, Emori S, Kainuma M, Kram, Meehl GA, Mitchell JF, Nakicenovic N, Riahi K, Smith SJ, Stouffer RJ, Thomson AM, Weyant JP, Wilbanks TJ. The next generation of scenarios for climate change research and assessment. *Nature*. 2010; 463(7282):747-56.
  23. Mearns Linda, McGinnis Seth, Korytina Daniel, Arritt Raymond, Biner Sebastien, Bukovsky Melissa, Chang Hsin-I, Christensen Ole, Herzmann Daryl, Jiao Yanjun, et al. *The NA-CORDEX dataset, version 1.0*. NCAR Climate Data Gateway, Boulder CO; 2017.  
[Accessed April 10, 2019]  
Available:https://doi.org/10.5065/D6SJ1JCH
  24. Taylor KE, Stouffer RJ, Meehl GA. An overview of CMIP5 and the experiment design. *Bull Am Met Soc*. 2012;93(4):485–498.

25. Schardong AA, Gaur SP, Simonovic, Sandink D. Computerized tool for the development of intensity-duration-frequency curves under a changing climate: Technical Manual v.3. Water Resources Research Report no. 103, Facility for Intelligent Decision Support, Department of Civil and Environmental Engineering, London, Ontario, Canada. 2018;67. [ISBN: 978-0-7714-3107-4]
26. Sandink D, Simonovic SP, Schardong A, Srivastav R. A decision support system for updating and incorporating climate change impacts into rainfall intensity-duration-frequency curves: Review of the stakeholder involvement process. Environmental Modelling & Software Journal. 2016;86:193–209. Available:doi.org/10.1016/j.envsoft.2016.06.012
27. Schardong A. Gaur, Simonovic SP, Sandink D. Computerized tool for the development of intensity-duration-frequency curves under a changing climate: User's manual v.3. Water Resources Research Report no. 104, Facility for Intelligent Decision Support, Department of Civil and Environmental Engineering, London, Ontario, Canada. 2018;80. [ISBN: 978-0-7714-3108-1]
28. Schardong A, Gaur A, Simonovic SP. Comparison of the theoretical Clausius-Clapeyron scaling and IDF\_CC tool for updating Intensity-Duration-Frequency Curves under climate change for Canada. J. Hydrol. Eng. 2018;23(9):04018036.
29. Olsson J, Berggren K, Olofsson M, Viklander M. Applying climate model precipitation scenarios for urban hydrological assessment: A case study in Kalmar City, Sweden. Atmos. Res. 2009;92:364–375. DOI: 10.1016/j.atmosres.2009.01.015
30. Bürger GG, Heistermann MM, Bronstert AA. Towards subdaily rainfall disaggregation via clausius-clapeyron. J. Hydrometeor. 2014;15:1303–1311. DOI: 10.1175/JHM-D-13-0161.1
31. Cannon AJ, Sobie SR, Murdock TQ. Bias correction of GCM precipitation by quantile mapping: How well do methods preserve changes in quantiles and extremes? Journal of Climate. 2015;28(17):6938–6959. DOI: 10.1175/JCLI-D-14-00754.1
32. IPCC: Annex I: Atlas of global and regional climate projections [van Oldenborgh GJ, Collins M, Arblaster J, Christensen JH, Marotzke J, Power SB, Rummukainen M, Zhou T. (eds.)]. In: Climate change: The physical science basis. Contribution of Working Group I to the Fifth Assessment Report of the Intergovernmental Panel on Climate Change [Stocker TF, Qin D, Plattner GK, Tignor M, Allen SK, Boschung J, Nauels A, Xia Y, Bex V, Midgley PM. (eds.)]. Cambridge University Press, Cambridge, United Kingdom and New York, NY, USA; 2013.
33. Sugahara S, Rocha RP, Silveira R. Non-stationary frequency analysis of extreme daily rainfall in Sao Paulo, Brazil. 2009;29:1339–1349. DOI: 10.1002/joc
34. Milly PCD, Betancourt J, Falkenmark M, Hirsch RM, Kundzewicz ZW, Lettenmaier DP, Stouffer RJ. Stationarity is dead: Whither water management? Science. 2008;319(5863):573-574.
35. Fortier C, Mailhot A. Climate change impact on combined sewer overflows. J. Water Resour. Plann. Manage. 2014;141: 04014073. DOI: 10.1061/(ASCE)WR.1943-5452 0000468, 04014073
36. Mailhot A, Duchesne S. Design criteria of urban drainage infrastructure under climate change. J. Water Resour. Plann. Manage. 2010;136(2):201-208. DOI: 10.1061/(ASCE)WR.1943-5452.0000023
37. Watt E, Marsalek J. Critical review of the evolution of the design storm event concept. Canadian Journal of Civil Engineering. 2013;40(2):105-113. DOI: 10.1139/cjce-2011-0594
38. Hosking J, Wallis J. Parameter and quantile estimation for the generalized pareto distribution. Technometrics. 1987; 29(3):339. DOI: 10.2307/1269343
39. Overeem A, Buishand A, Holleman I. Rainfall depth-duration-frequency curves and their uncertainties. Journal of Hydrology. 2007;348(1-2):124-134. DOI: 10.1016/j.jhydrol.2007.09.044
40. Millington N, Das S, Simonovic SP. The comparison of GEV, log-pearson type 3 and gumbel distributions in the upper thames river watershed under global climate models. Water Resources Research Report no. 077, Facility for Intelligent Decision Support, Department of Civil and Environmental Engineering, London, Ontario, Canada. 2011;53.

41. Provost SB, Saboor A, Cordeiro GM, Mansoor M. On the q-Generalized extreme value distribution REVSTAT – Statistical Journal. 2018;16(1):45–70.
42. Nguyen VTV, Nguye TD, Cung A. A statistical approach to downscaling of sub-daily extreme rainfall processes for climate-related impact studies in urban areas. Water Science & Technology: Water Supply. 2007;7(2):183-192.
43. Paixao E, Auld H, Mirza MMQ, Klaassen J, Shephard MW. Regionalization of heavy rainfall to improve climatic design values for infrastructure: A case study in Southern Ontario, Canada, Hydrol. Sci. J. 2011;56: 1067–1089.  
DOI: 10.1080/02626667.2011.608069
44. Ganguli P, Coulibaly P. Does nonstationarity in rainfall require nonstationary intensity–duration–frequency curves? Hydrol. Earth Syst. Sci. 2017;21:6461–6483.  
DOI: 10.5194/hess-21-6461-2017
45. ECCC: Environment and climate change canada, intensity-duration-frequency (IDF) Files v3.0,  
Available:[http://climate.weather.gc.ca/prods\\_servs/engineering\\_e.html](http://climate.weather.gc.ca/prods_servs/engineering_e.html)  
(Last access: April 10, 2019)

## APPENDIX I – List of GCMs in the IDF\_CC Tool

Country	Centre Acronym	Model	Centre Name	Number of Ensembles (PPT)	GCM Resolutions (Lon. vs Lat.)
China	BCC	bcc_csm1_1	Beijing Climate Center, China Meteorological Administration	1	2.8 x 2.8
China	BCC	bcc_csm1_1 m	Beijing Climate Center, China Meteorological Administration	1	
China	BNU	BNU-ESM	College of Global Change and Earth System Science	1	2.8 x 2.8
Canada	CCCma	CanESM2	Canadian Centre for Climate Modeling and Analysis	5	2.8 x 2.8
USA	CCSM	CCSM4	National Center of Atmospheric Research	1	1.25 x 0.94
France	CNRM	CNRM-CM5	Centre National de Recherches Meteorologiques and Centre Europeen de Recherches et de Formation Avancee en Calcul Scientifique	1	1.4 x 1.4
Australia	CSIRO3.6	CSIRO-Mk3-6-0	Australian Commonwealth Scientific and Industrial Research Organization in collaboration with the Queensland Climate Change Centre of Excellence	10	1.8 x 1.8
USA	CESM	CESM1-CAM5	National Center of Atmospheric Research	1	1.25 x 0.94
E.U.	EC-EARTH	EC-EARTH	EC-EARTH	1	1.125 x 1.125
China	LASG-CESS	FGOALS_g2	IAP (Institute of Atmospheric Physics, Chinese Academy of Sciences, Beijing, China) and THU (Tsinghua University)	1	2.55 x 2.48
USA	NOAA GFDL	GFDL-CM3	National Oceanic and Atmospheric Administration's Geophysical Fluid Dynamic Laboratory	1	2.5 x 2.0
USA	NOAA GFDL	GFDL-ESM2G	National Oceanic and Atmospheric Administration's Geophysical Fluid Dynamic Laboratory	1	2.5 x 2.0
USA	NOAA GFDL	GFDL-ESM2M	National Oceanic and Atmospheric Administration's Geophysical Fluid Dynamic Laboratory		2.5 x 2.0
United Kingdom	MOHC	HadGEM2-AO	Met Office Hadley Centre	1	1.25 x 1.875
United Kingdom	MOHC	HadGEM2-ES	Met Office Hadley Centre	2	1.25 x 1.875
France	IPSL	IPSL-CM5A-LR	Institut Pierre Simon Laplace	4	3.75 x 1.8
France	IPSL	IPSL-CM5A-MR	Institut Pierre Simon Laplace	4	3.75 x 1.8
Japan	MIROC	MIROC5	Japan Agency for Marine-Earth Science and Technology	3	1.4 x 1.41
Japan	MIROC	MIROC-ESM	Japan Agency for Marine-Earth Science and Technology	1	2.8 x 2.8

Country	Centre Acronym	Model	Centre Name	Number of Ensembles (PPT)	GCM Resolutions (Lon. vs Lat.)
Japan	MIROC	MIROC-ESM-CHEM	Japan Agency for Marine-Earth Science and Technology	1	2.8 x 2.8
Germany	MPI-M	MPI-ESM-LR	Max Planck Institute for Meteorology	3	1.88 x 1.87
Germany	MPI-M	MPI-ESM-MR	Max Planck Institute for Meteorology	3	1.88 x 1.87
Japan	MRI	MRI-CGCM3	Meteorological Research Institute	1	1.1 x 1.1
Norway	NOR	NorESM1-M	Norwegian Climate Center	3	2.5 x 1.9

© 2019 Schardong and Simonovic; This is an Open Access article distributed under the terms of the Creative Commons Attribution License (<http://creativecommons.org/licenses/by/4.0>), which permits unrestricted use, distribution, and reproduction in any medium, provided the original work is properly cited.

*Peer-review history:*  
 The peer review history for this paper can be accessed here:  
<http://www.sdiarticle3.com/review-history/49512>